VPH gratings technology for the Thirty Meter Telescope instrumentation program

John S. Pazder[*a], J .Christopher Clemens[b]

[a]National Research Council Canada, Herzberg Institute of Astrophysics, 5071 West Saanich Road, Victoria, BC, Canada, V9E 2E7
[b]Department of Physics and Astronomy, University of North Carolina, Chapel Hill, NC 27599

ABSTRACT

Volume Phase Holographic Gratings (VPHG) provide unique advantages over traditional dispersive elements and are being considered for instruments on many large telescopes, including the Wide Field Optical Spectrograph (WFOS) for the Thirty Meter Telescope (TMT). In this paper we review the properties of VPHG particularly with regard to their use in large multi-object spectrographs such as WFOS. Design considerations include optimal sizes and working angles, and variations in blaze efficiencies as a function of grating and field angles. For instruments like WFOS, a gratings mosaic is a promising solution to meet the size requirements. The methodologies of mosaics and the required tolerances are evaluated. VPH gratings may also be used in echelette mode with significant advantages, although more lab tests should be carried out to explore and optimize performance. A brief status report on the VPHG development activities in the Goodman lab is included, with a plan for future development.

Keywords: Thirty Meter Telescope, Volume Phase Holographic, VPH, VPHG, gratings, spectrograph, Goodman lab

1. INTRODUCTION

As part of the Thirty Meter Telescope (TMT) instrumentation program, we have been studying the application of Volume Phase Holographic Grating (VPHG) for use on TMT. The VPHG and its application in astronomy is discussed by Barden[1], [2]. The reader is referred to these papers for background on the VPHG. The advantages of the VPHG are significant and Robertson[3] gives an excellent summary of these. One of the instruments for which we have been considering the application of the VPHG is the TMT Wide-Field Optical Spectrograph (WFOS), one of the TMT early light instruments[4]. We repeat here some of the key advantages for the VPHG over conventional ruled reflection gratings:

- higher efficiency (80% to 90% for VPH versus 60% to 70% for ruled reflection gratings)
- smaller exit pupil distances for the camera and collimators for VPHs (as they are transmission gratings)
- Littrow configurations possible, (allowing no anamorphic magnification giving smaller camera optics)
- VPHG's are made to order, allow optimal line density and blaze
- blaze of VPHG can be shifted, tuning the highest efficiency to wavelength range of interest

These gratings are not without disadvantages and challenges. To realize the full benefits of the VPHG, articulation of cameras is needed, adding complexity and cost to the mechanical design. The VPHGs of the size needed for TMT represent the cutting edge or beyond of VPHG manufacturing technology. VPHGs used in multi-order 'echellette' mode have been proposed but are unproven on the sky[3], [5]. Because of these disadvantages and challenges, the current TMT WFOS concept is based on reflection grating[6]. We present the results of our investigation into VPHGs for a WFOS on TMT and recent development work at the Goodman Laboratory to develop larger VPHGs.

* John.Pazder@nrc-cnrc.gc.ca

2. VPHG SIZING FOR MULTI-OBJECT SPECTROGRAPHS

The most significant trade in VPHG spectrograph design is between the pupil size and maximum allowable working angle at the grating. In the context of TMT, this trade is critical. To achieve the same slit-width-Resolution product ($\phi_w R$) with a seeing limited spectrograph on a 30m class telescope, the dispersive element needs to introduce three times the path difference as on a 10m. This requires either larger grating or larger working angles, or both. A larger grating imposes stiff penalties in cost, weight and complexity for the instrument. The preferable solution is the smallest grating with the largest working angles to satisfy the requirements.

Solutions which deviate greatly from Littrow can give larger resolutions with the same collimator pupil diameter. Unfortunately, this introduces anamorphic magnification, resulting in a wider grating and a larger (and faster) camera. The Littrow configuration is a better balance of complexities. It is the maximum resolution for a given deviation angle (collimator to camera angle) with a grating of a fixed width. We explored the maximum resolution achievable with efficient operation at Littrow with the VPHG. We analyzed only the Littrow case with un-slanted fringes but we are aware that to minimize grating ghosts the spectrograph will have to operate slightly outside this area as discussed by Burgh[7].

For a seeing limited astronomical spectrograph, the resolution (R) at Littrow is given by

$$R = \frac{2d_{col}\tan(\alpha)}{\phi_w D_{tel}}$$

Where d_{col} is the collimator exit pupil diameter, D_{tel} is the telescope diameter, ϕ_w is the slit width, and α is incident angle on the grating.

. The penalty for increasing R by enlarging the pupil is higher cost, as mentioned above, while the penalty for increasing R by using larger incident angle is lower efficiency. The relevant costs of larger pupils are generally familiar to designers of opto-mechanical systems, but the efficiency losses at the VPHG with larger grating angles are not. As the working angle of the grating is increased, the gain in resolution is offset by a drop in efficiency due to polarization effects at the grating. Rigorous coupled wave analysis (RCWA) of various model diffraction gratings shows that peak efficiency scales solely with working angle (in air). Figure 1 presents the RCWA-derived values for the peak efficiency for un-polarized light as a function of incident angle (α).

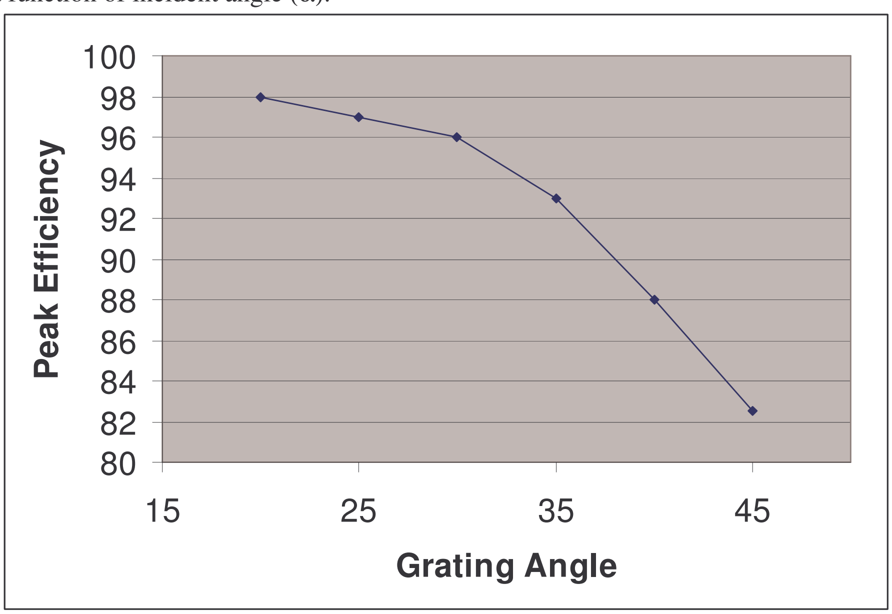

Figure 1: The drop in VPH efficiency maxima at large working angle due to polarization effects (surface reflection losses are not included).

It is possible to design narrow bandwidth gratings (Dickson gratings) that circumvent these efficiency losses, but these are not general purpose devices and we do not consider them for a general purpose spectrograph.

An additional efficiency loss associated with the higher working angles arises because, at a fixed wavelength, higher line density is required to achieve the same resolving power. Higher line density makes the grating bandwidth narrower, increasing the loss at the edges of the wavelength coverage on the detector. This effect is shown in Figure 2 for two different trades between pupil size and maximum working angle. In this example, the system demagnification was kept constant, i.e. the collimator and camera focal lengths were changed by the same fraction. The average efficiency degradation in this example is about 50% greater than the decrease in peak efficiency (a 15% loss rather than 10%).

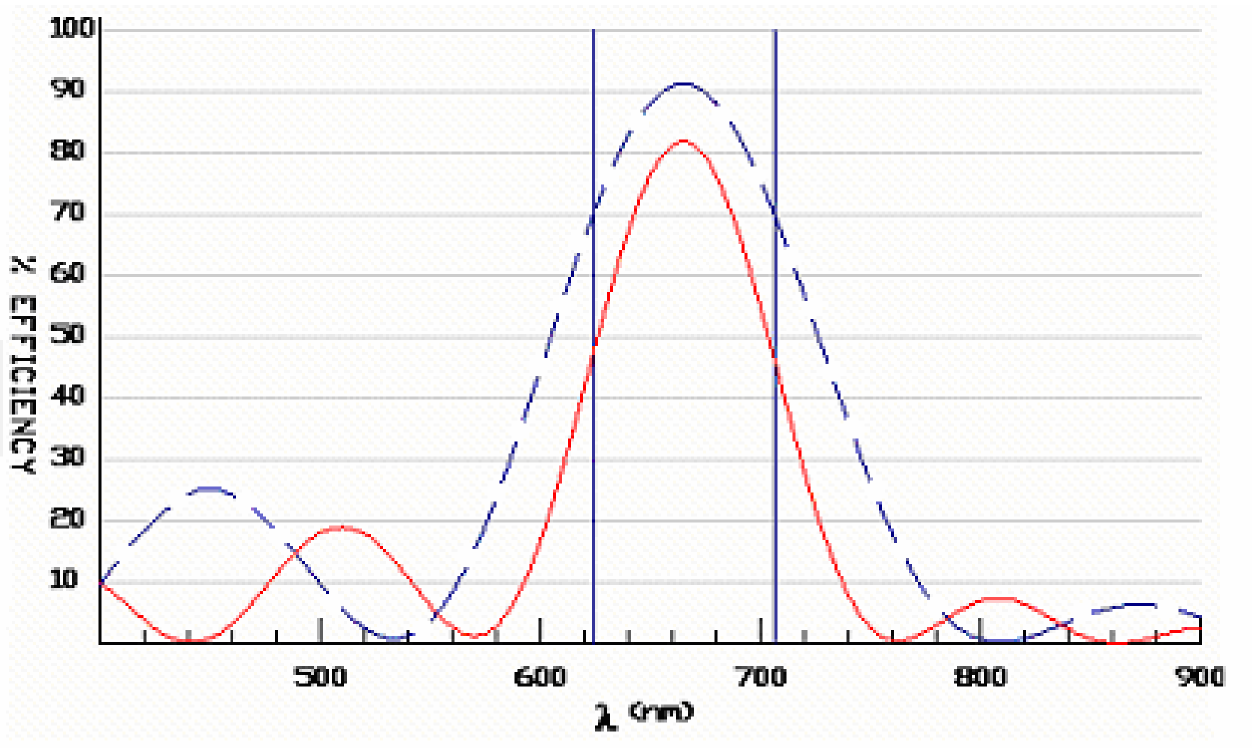

Figure 2: Efficiency curve for a 400 mm pupil WFOS at maximum working angle of 37 degrees (1800 l/mm grating, dashed blue line) and the same curve for a 300 mm pupil WFOS at a maximum working angle of 45 degrees (2120 l/mm grating, solid red line). The bars denote typical CCD coverage, which is the same in each case because the camera f ratio was held constant.

The temptation is often to push the pupil size to its maximum conceivable value to get the highest grating diffraction efficiency and band width at the high resolution range. However, larger pupils incur stiff penalties in cost, weight, and complexity. The low resolution limit for the spectrograph is also an important consideration with the pupil size. A larger pupil will impose a lower line frequency for the low resolution range. For low line density gratings, the peak efficiency as a function of field angle (the super-blaze) drops rapidly with field angle limiting the performance. In addition, there is a thickness limit of the dichromate gel layer in the VPHG which is usable, further limiting the low resolution range.

A more sensible approach is to design the smallest pupil size which meets the requested specifications without significant efficiency losses. A grating working angle of about 35 degrees is at the knee of the drop in efficacy, giving an optimal balance between pupil size and loss. At this angle, peak diffraction efficiency is greater than 90%.

To achieve a resolution of 5000 with a 0.75" slit at a grating working angle of 35 degrees on TMT, the required grating size is 400mm x 490mm with a 400mm collimator pupil on the spectrograph. Currently, no VPHG vendor is able to produce a monolithic VPHG of this size. CSL-ATHOL has produced the largest monolith astronomical grating of

380mm diameter[8]. It is conceivable to design for a slightly smaller pupil size of 380mm, but a second possibility of using a grating mosaic is also very attractive. Grating mosaics are discussed in detail in section 5.

If possible, allowing articulation of the camera to 90 degrees to keep the option open for a higher resolution mode of R~7500 with reduced (10% to 15%) efficiency should be considered. For the remainder of this paper, we consider a spectrograph of these specification (a 400mm collimator pupil) with a 4.5’x4.5’ slit mask and 9’x4.5’ detector field of view.

The diffraction efficiency at R5000 is plotted in Figure 3. The solid-green lines represent center field, and the long-dashed-red and short-dashed-blue lines represent spectra from the extreme left and right field angles for a 4.5 minute slit masks and 9 minute detector width in the dispersion direction. The bars denote the CCD coverage for the respective fields. The blaze shift with field angle can be seen in this figure. Section 3 shows the blaze shift effect is independent of the VPHG size and the grating working angle.

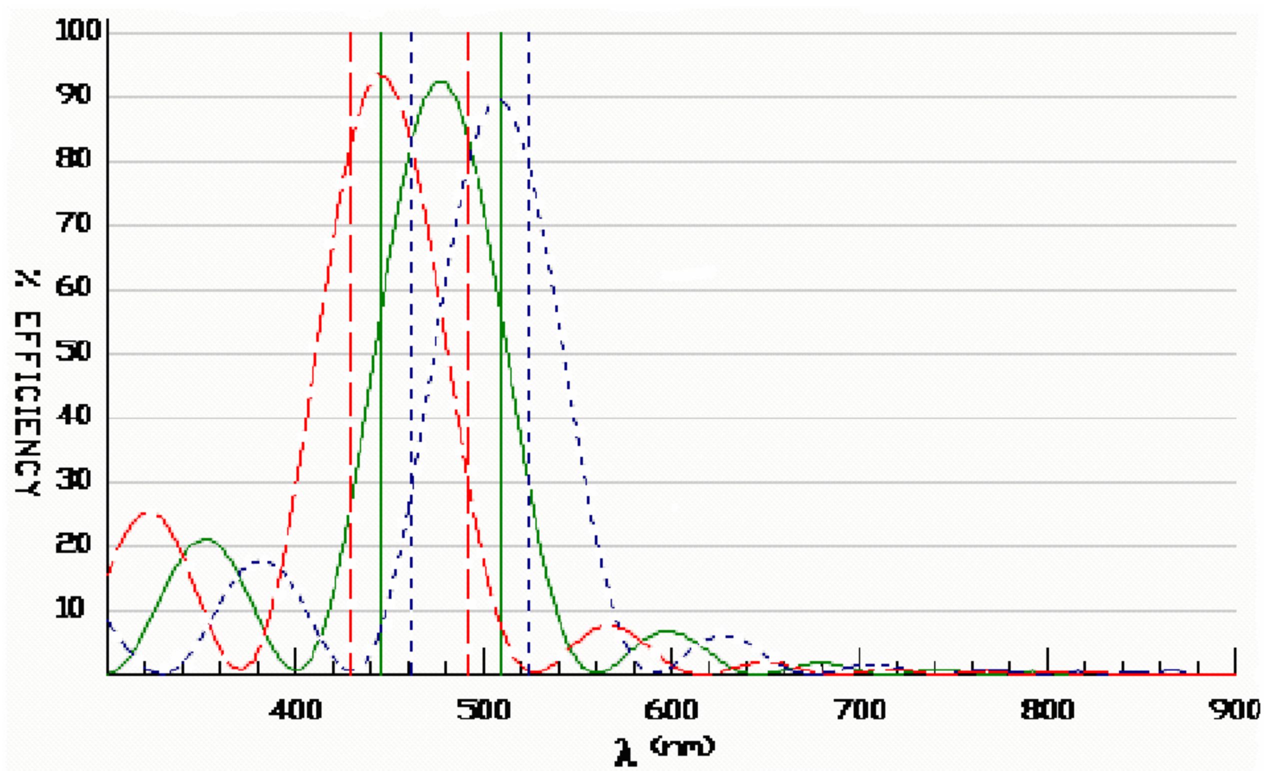

Figure 3: VPH diffraction efficiency at R5000 across the slit mask field (400mm grating/35 degree grating working angle) The solid-green lines represent center field, and the long-dashed-red and short-dashed-blue lines represent spectra from the extreme left and right field angles for a 4.5 minute slit masks and 9 minute detector width in the dispersion direction. The bars denote the CCD coverage for the respective fields.

To complete the discussion of VPHG efficiencies, it is worth while to consider reflection losses at the air glass surfaces. Calculations are show in Figure 4 for a single layer sol-gel coating and a 3 layer coating at 35 degrees and 45 degree incidence. Losses are less than 0.2% per air-glass surface over a 100nm with the sol-gel coating. Sol-gel has very low stress and can be applied to large optics with the spin coating process[9]. A more complicated coating can be used if a wider band pass is required. An example is given of the performance for a “3 layer” coating with less than 0.5% at 35 degrees and 1% at 45 degrees over 200nm.

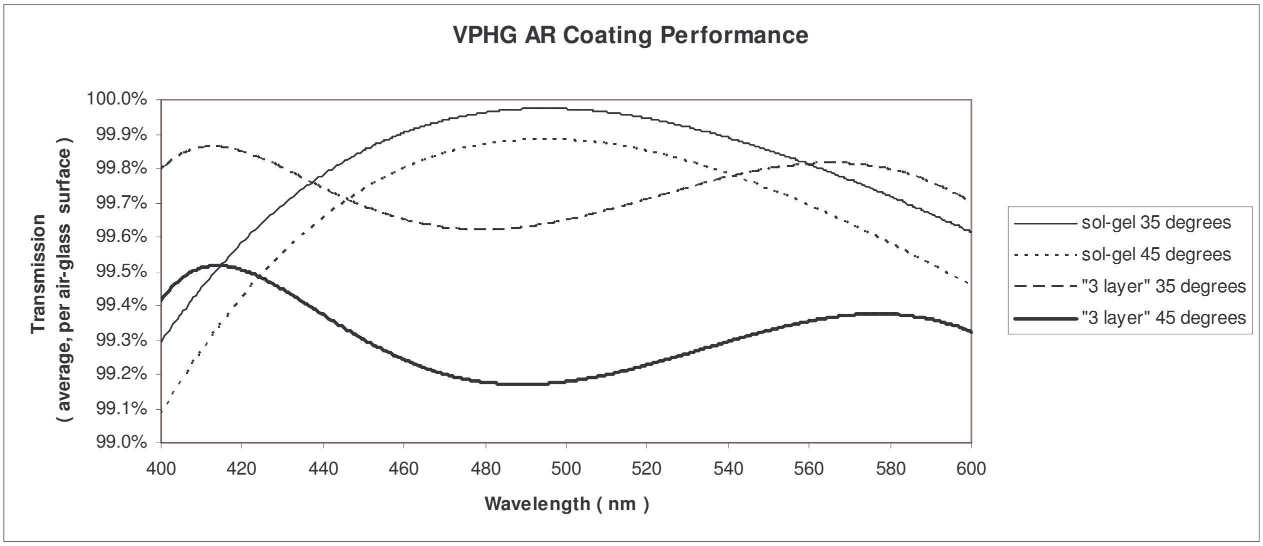

Figure 4: VPHG anti-reflection coating performance for sol-gel and '3 layer' coatings at 35 and 45 degrees for substrate of index 1.5. Transmission is per air-glass surface for un-polarized light.

3. VPH BLAZE SHIFT WITH FIELD ANGLE

The blaze of the VPHG is characteristically different than the blaze for ruled gratings in that it can be tuned by changing the incident angle. This property can be utilized to tune the blaze to a particular region of interest to improve spectrograph efficiency and extend the useful operating range of a particular grating. For a multi-object spectrograph, this VPHG characteristic introduces additional complexity in the diffraction efficiency because the blaze wavelength shifts across the field of view of the slit mask as shown in Figure 3.

Robertson[3] gives an excellent discussion of blaze shift with field angle across the slit mask and presents a simple equation for calculating this shift. The equation is good in agreement without results over our range of spectrograph parameters (within 10% of RCWA analysis) and is sufficient for characterizing this effect. This equation expressed in terms of a shift from the Littrow blaze wavelength ($\lambda_{Littrow}$) is

$$\lambda_{BlazePeak} = \lambda_{Littrow}\left[1+\frac{(D_{tel}/d_{col})\Delta\theta}{\tan(\alpha_{Littrow})}\right]$$

where $\Delta\theta$ is the field angle (on the sky, in radians) of the off axis object, D_{tel} is the telescope diameter, d_{col} is the collimator exit pupil diameter, and $\alpha_{Littrow}$ is incident angle on the grating for the on-axis slit. To understand this blaze shift we compare it to the wavelength at the center of the detector for the same field angle. The wavelength at the center of the detector for an off axis object is

$$\lambda_{\det ector\_center} = \frac{\lambda_{Littrow}}{2}\left[1+\frac{\sin(\alpha_{Littrow}+\Delta\alpha)}{\sin(\alpha_{Littrow})}\right] \cong \lambda_{Littrow}\left[1+\frac{(D_{tel}/d_{col})\Delta\theta/2}{\tan(\alpha_{Littrow})}\right]$$

The approximation on the right is within a percent for $\Delta\alpha$ less than 8 degrees, and thus is a valid approximation for contemporary multi-object astronomical spectrographs because of the limits of the current camera optical designs.

Comparing these equations, we see the blaze shift is simply twice the wavelength shift at the center of the detector. It can be further shown that the blaze peak will shift a constant proportion across the detector independent of resolution and wavelength. The blaze peak will shift from the center of the detector by 1/(2r) of the detector width. The term r is the ratio of detector width to slit mask width in the dispersion direction. Typically, r is chosen to be ~2; in this case, the blaze will shift by ¼ of the detector width. For ruled gratings, the blaze does not shift in wavelength, but the wavelength at the center of the detector does shift with slit position. The net effect is the blaze peak for ruled gratings shifts by the same amount on the detector, but in the opposite direction. Blaze shift with field angle is show in Figure 5 and Figure 6, illustrating this effect for the case of r=2. Also indicated on the plots is the change of FWHM of the VPHG diffraction efficiency. This does scale with λ and R, increasing with λ, and decreasing with R.

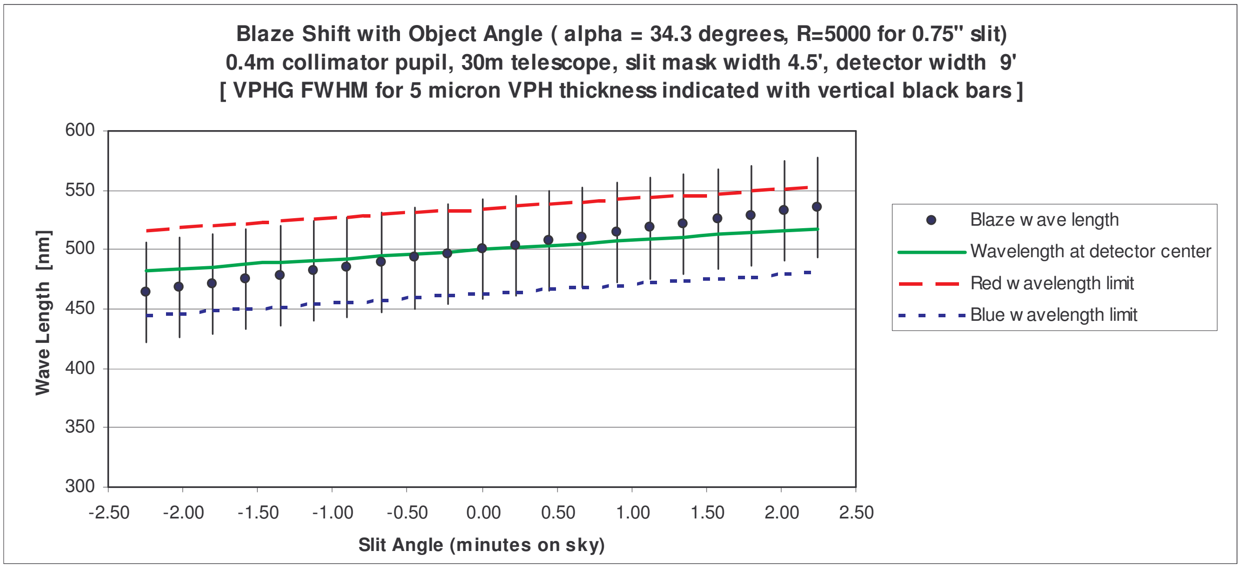

Figure 5: Blaze Shift with Object Angle (R5000). CCD coverage is denoted with long-dashed red line and short dashed blue line and a solid-green line for the wavelength at the center of the detector. The blaze wavelength is indicated with the dots. The vertical bars indicate the FWHM of the VPHG diffraction efficiency.

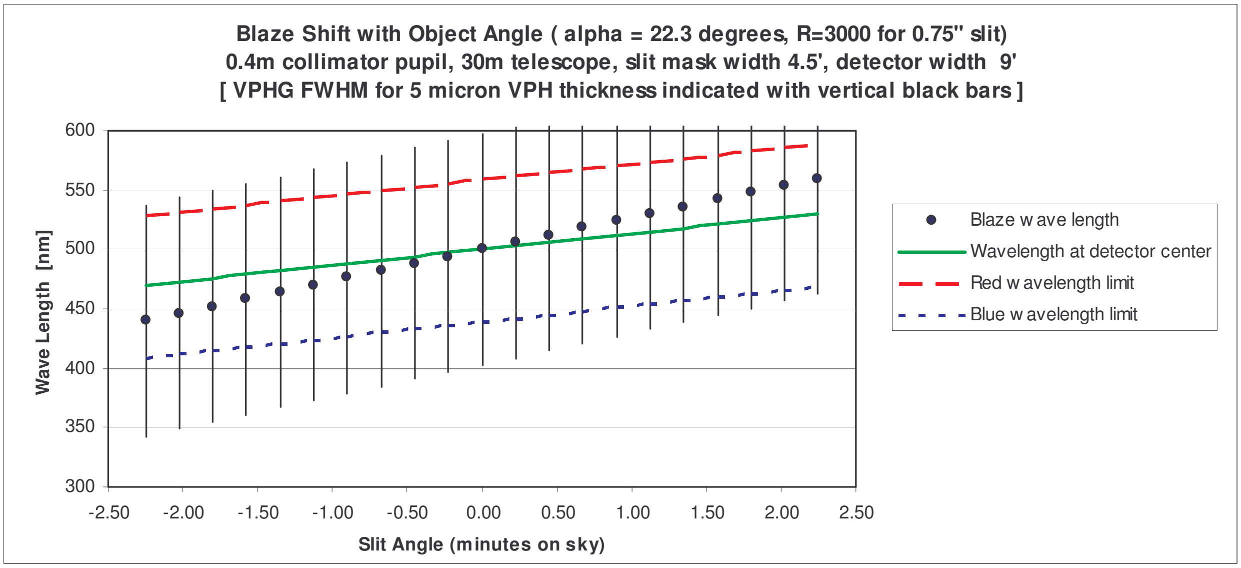

Figure 6: Blaze Shift with Object Angle (R3000). CCD coverage is denoted with long-dashed red line and short dashed blue line and a solid-green line for the wavelength at the center of the detector. The blaze wavelength is indicated with the dots. The vertical bars indicate the FWHM of the VPHG diffraction efficiency.

4. VPHG MULTI-ORDER EFFICENCY

The performance of VPHG at diffraction orders up to 5 for 'echellette' type modes has been modeled and measured by Barden[5]. Measurements of a 300 l/mm grating showed better-than-theory performance with diffraction efficiencies better than 60% up to order 3. This was explainable only by assuming a distorted or quasi-sinusoidal index profile in the gratings. Subsequent modeling was done to design an 'echellette' grating with the quasi-sinusoidal index profile. The predicted efficiencies were favorable, >60% up to order 8 but unfortunately the grating did not perform as well as theory, only > 50% up to order 4. Although this work is promising, even better control of the fringe structure is required to manufacture a high efficiency high order VPH 'echellette'.

Ebizuka[10] has designed a "Quasi-Bragg grating" as another approach to a high order performance with a VPH like grating. This grating is unlike a normal VPHG in that, rather than a sinusoidal grating index modulation, it is formed of a stack of mirrors aligned like a window blind. The performance of this "Quasi -Bragg grating" is excellent, with better than 75% diffraction efficiency from the 6^{th} to 15^{th} order. Ebizuka has build prototype gratings which work as predicted but performance is limited due to imperfections in the fabrication.

Theoretically, a high efficiency 'echellette' VPHG is possible, but gratings such as these are still under development.

5. VPHG MOSAICS

With VPHG Mosaics it is possible to produce VPHG as large as needed. Using a 2x2 mosaic would allow all of the VPHG labs to produce 400mm sized gratings with their existing recoding setup apertures. For these reasons, we have considered carefully the possible ways of producing mosaics and the manufacturing tolerances required for a WFOS on TMT.

A NxN VPH mosaic can be built $N/\sqrt{2}$ larger than the largest monolithic diameter that can be recorded. Grating mosaics are not new; mosaics have been built from ruled reflection grating for astronomical spectrographs for decades. For VPHGs, this technique has been demonstrated by the construction of two 340mmx240mm 2x2 VPHG mosaics by CSL-ATHOL[8]. With existing recording capabilities, a 400mm VPHG can be produced today with a 2x2 mosaic but such a grating is not without challenge.

VPHG mosaics are a similar challenge to ruled reflection mosaics. Micron level precision opto-mechanics are required to produce and align the grating. To understand the challenges we have examined the alignment and manufacturing tolerances for a 400mm x 490mm VPHG mosaic on TMT (D_{tel}= 30m) in Littrow operating at a resolution slit-width product ($\mathscr{R}\phi$) of 5000x0.75" or 3750" (thus α = 34.3 degrees). We assume a system level image quality tolerance of 0.2" on the sky for the spectrograph. For a seeing limited instrument we are not diffraction limited so it unnecessary to phase the gratings together, considerably loosening the required tolerances as the grating is insensitive to in plane linear motions and thickness of the encapsulating windows. Additionally, the grating being transmissive and in Littrow means the grating is insensitive to grating rotation in the plane of dispersion and grating tip perpendicular to this plane. To produce an error of 0.02" ($1/10^{th}$ of the system level tolerance) the corresponding perturbation in grating rotation and tilt are 0.2 and 2 degrees respectively.

The remaining tolerances (groove frequency, wedge, and clocking) are sensitive. For these, we calculate the tolerance for an image quality degradation of $\Delta\phi$=0.04" on the sky. This corresponds to $1/5^{th}$ of the system level image quality, a good rule of thumb for a top down partition of dominant error terms in a system. The groove frequency tolerance is resolution dependent and given by $\Delta\phi/(\mathscr{R}\phi)$: for our example, the tolerance is approximately 1 part in 100 thousand. This will require careful process control in production. It will be desirable to expose all sections of the mosaic under the same optical setup, without changes in the alignment of the optics and ideally on the same day. For example, a grating rotation error of 3 arcseconds on the recording setup will cause a 1 part in 100 thousand groove frequency error, but it is the repeatability and not the absolute error of the setup that must meet this specification. A differential mechanical wedge of $\Delta\theta$ from mosaic element to mosaic element will cause an on sky image error of $\Delta\phi = (n-1)\Delta\theta\ d_{grating}/D_{tel}$. For our allocation of $\Delta\phi$=0.04" the mechanical wedge is 6" or 6 microns over the mosaic element size of 200mm. Monitoring of optical beam deviation to control wedge during encapsulation will be necessary. Grating clocking is the remaining sensitive tolerance. We define clocking ($\Delta\xi$) as rotation in the plane of the grating. An error of image motion perpendicular to the dispersion results from grating clocking. This is again resolution dependent and the on sky image error is given by

$$\Delta\phi = 2\alpha \frac{d_{grating}}{D_{tel}} \sin(\Delta\xi)$$

For our allocation of Δϕ=0.04" the corresponding grating clocking tolerance is $\Delta\xi$ = 2.5 arcseconds or 2.5 microns over a mosaic element size of 200mm. Fortunately, this parameter is easy to measure by diffracting a laser beam over a long baseline. This necessary adjustments to achieve this tolerance require precision opto-mechanical alignment jigs.

Three methods have been identified for building VPH mosaics: framed, common bonded, and step & repeat. These methods are illustrated in Figure 7. Framed mosaics are individual VPHGs fabricated and encapsulated individually and framed together with an external support structure. This simplifies the VPHG production, but adds complexity in the external support structure. The obscuration from the mosaic boundaries for a 400mmx490mm 2x2 mosaic is estimated to be less than 2%. As shown in the figure, the boundaries between the mosaic elements are beveled to the incident angles on the grating to minimize the obstruction. For mosaics larger than 2x2, the obscuration will be considerably larger as the elements can not be edge supported.

In the common bonded approach, the mosaic elements are fabricated individually but are bonded to a common substrate in the encapsulation process. This eliminates the need for the frame but complicates the bonding process with the added precision for the mosaic element alignment. The obscuration for this approach is estimated to be less than 1%.

The step and repeat used a single substrate which is exposed in sub-sections. No enlargement is required of the recording optics, but the DGH coating and processing must be able to handle the full size of the mosaic. The light loss is potentially much smaller, ~ 0.25%, but the technical challenges are considerably more severe.

The common bonded method is perhaps the best method for VPHG mosaics. The CSL mosaics were of this type. This method is readily adaptable to 3x3 or larger mosaics and, once fabricated, there is no risk of misalignment as in the framed method.

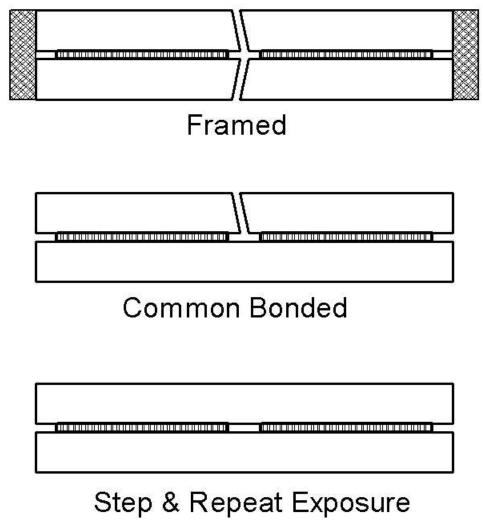

Figure 7: Side profiles of 3 mosaicking methods. **Top:** framed mosaic where four independent gratings are head in place by a frame around the edges. **Center:** common bonded method where VPHGs are fabricated independently and bonded to a common substrate. **Bottom:** Step & Repeat where a monolithic substrate is exposed in

6. RECENT DEVELOPMENT WORK AT THE GOODMAN LABORATORY

The Goodman laboratory has been developing the ability to coat, expose and process gratings made on substrates up to 305 mm in size. The equipment available for production consists of a spin coater capable of accepting substrates up to 1 m in size, a 25 W Argon-Ion laser, an optical bench with two 350mm off-axis parabolic collimators and two 400mm precision optical steering flats, and process tanks capable of processing plates up to 600mm in size. Our current efforts have concentrated upon producing scientific quality gratings that are 200 mm x 250 mm in size. We have successfully produced quality gratings of 1600 and 700 l/mm, but the yield is low. The problems contributing to low yield are summarized below.

Process Step	Yield	Causes of Failure
Spin Coating	50%	Voids, impurities, inclusions, operator error, high lab humidity
Drying	99%	Handling errors
Holographic Exposure	50%	Air movements, creep, bubbles in coupling fluid, laser problems
Processing	75%	Handling problems with large substrates, high lab humidity

The resulting total yield for our process is about 18%, so only about one in five gratings is presentable enough to encapsulate.

We have developed a unique characterization facility that provides automated measurements of the zeroth order transmitted spectrum at numerous angles and compares these to rigorous coupled wave models. This allows us to measure gratings within five minutes after they are produced and to adjust the processing of subsequent gratings in the same batch to hit our blaze target.

The main impediment to progress has been retaining skilled personnel. It requires months of training to learn the necessary skills to make good gratings, and not all of the technicians we have hired have been able to do it successfully. The loss of key personnel after training can reduce our yield to zero for months. We are addressing this problem by trying to keep two production personnel at all times to provide continuity.

7. ROADMAP FOR FUTURE DEVELOPMENT AT THE GOODMAN LABORATORY

The Goodman Laboratory development effort has relied upon sporadic internal funding, but our current plan is to raise sufficient funds to keep operations running smoothly. This would be easier if there was a promise of commercialization of the technology, but the market for large VPH gratings does not support any commercialization plan we have been able to construct. It is going to require funding of approximately $200K per year to develop and maintain the ability to produce large gratings for astronomical use, and we plan to raise this from state, federal, and observatory sources.

Our efforts to produce single gratings of 200 x 250 mm gratings are 90% complete. In July 2008, we will move our laboratory to a larger facility that has humidity control and new coating equipment. This should increase the yield and the repeatability of our process. Once we are consistently producing single gratings, we will attempt to incorporate them into mosaic structures. This will require the construction of alignment jigs and appropriate optical alignment tools. We expect the first of these in early 2009.

8. CONCLUSIONS

We have explored the use of VPH gratings for use in the TMT Wide Field Optical Spectrograph and other large multi-object spectrographs. Our analysis indicates that the optimal grating working angle for such VPHG spectrographs is approximately 35 degrees. The corresponding collimator pupil size for R5000 at 0.75” slit width is 400mm. At R5000 the theoretical diffraction performance will be greater than 90% at the blaze peak, 85% average. Monolithic VPH gratings close to this size have been produced, but VPHG mosaics offer the possibility of producing gratings of the required size, or larger. The Goodman laboratory is continuing to investigate the methods to improve the performance and is especially well suited to the development of large VPHG and VPHG mosaics.

ACKNOWLEDGMENTS

The authors gratefully acknowledge the support of the TMT partner institutions. They are the Association of Canadian Universities for Research in Astronomy (ACURA), the California Institute of Technology and the University of California. This work was supported as well by the Gordon and Betty Moore Foundation, the Canada Foundation for Innovation, the Ontario Ministry of Research and Innovation, the National Research Council of Canada, and the U.S. National Science Foundation.

REFERENCES

[1] Barden, S.C., Arns, J.A. and Colburn, W.S., “Volume-phase holographic gratings and their potential for astronomical applications”, Proc. SPIE 3355, pp.866-876 (1998).
[2] Barden, S.C., Arns, J.A. and Colburn, W.S., “Astronomical applications of volume phase holographic grating”, Proc. SPIE 3749, pp.52-53 (1999).
[3] Robertson, J.G, Taylor K., Baldry, I.K., Gillingham, P.R., and Barden, S.C., “Atlas: a cassegrain spectrograph based on volume holographic gratings”, Proc. SPIE 4008, pp. 194-202 (2008)
[4] Crampton, D, Simard, L., and Silva, D., “Early Light TMT Instrumentation”, Proc. SPIE 7014, (2008)
[5] Barden, S.C., Arns, J.A. Colburn, W.S., and Williams, J.B., “Evaluation of volume-phase holographic technology”, Proc. SPIE 4485, pp. 429-438 (2002)
[6] Bernstein, R. and Bigelow, B., “Optical Design of a Wide Field Optical Spectrograph for TMT”, Proc. SPIE 7014, (2008)
[7] Burgh, E.B., Bershady, M.A., Westfall, K.B., and Kenneth, H,N, “Recombination Ghosts in Littrow Configuration: Implications for Spectrographs Using Volume Phase Holographic Gratings”, PASP,119, p.p.1069-1082 (2007)
[8] Blanche, P.-A., Gailly, P., Habraken, S., Lemaire, P., and Jamar, C., “Mosaiced and high line frequency VPH gratings for astronomy”, Proc. SPIE 5494, pp. 208-216 (2004)
[9] Stilburn, J. R., “High-efficiency sol-gel antireflection coatings for astronomical optics”, Proc. SPIE 4008, pp. 1361-1367 (2000)
[10] Ebizuka, N., et al., “Novel Immersion Gratings, VPH Gratings and Quasi-Bragg Gratings”, Proc. SPIE 6273, 62732G (2006)